

Effects of an in-plane magnetic field on c -axis sum rule and superfluid density in high- T_c cuprates

Wonkee Kim and J. P. Carbotte

Department of Physics and Astronomy, McMaster University, Hamilton, Ontario, Canada

L8S 4M1

Abstract

In layered cuprates, the application of an in-plane magnetic field (\mathbf{H}) changes the c -axis optical sum rule and superfluid density ρ_s . For pure incoherent c -axis coupling, \mathbf{H} has no effect on either quantities but it does if an additional coherent component is present. For the coherent contribution, different characteristic variations on \mathbf{H} and on temperature result from the constant part (t_{\perp}) of the hopping matrix element and from the part (t_{ϕ}) which has zero on the diagonal of the Brillouin zone. Only the constant part (t_{\perp}) leads to a dependence on the direction of \mathbf{H} as well as on its magnitude.

PACS numbers: 74.20.-z,74.25.Gz

A conventional c -axis optical sum rule¹ has been observed in some high- T_c cuprates such as optimally doped YBCO,² while in others, such as underdoped YBCO, it is violated. The sum rule is formulated in terms of the missing area at finite energy ω under the real part of the optical conductivity when the sample becomes superconducting. In the conventional case this missing spectral weight (ΔN) shows up as the superfluid density (ρ_s) at zero energy and $\Delta N/\rho_s = 1$. Underdoped YBCO exhibits a pseudo gap above the superconducting critical temperature (T_c). This is taken as an indication of non-Fermi liquid in-plane behavior and $\Delta N/\rho_s \simeq 1/2$. Even for an in-plane Fermi liquid, deviations³ from one result for $\Delta N/\rho_s$ if the c -axis coupling is incoherent, *i.e.* does not conserve in-plane momentum. On the other hand, the conventional value of $\Delta N/\rho_s$ observed in optimally doped YBCO is consistent with an in-plane Fermi liquid and coherent c -axis dynamics³ whether or not the hopping amplitude depends on in-plane momentum. It is clear, therefore, that such measurements can yield important information on the dynamics of the charge carriers in the cuprates.

Information on the nature of the interlayer coupling can also be obtained from other measurements. For example, it was recognized⁴ that the temperature (T) variation of the c -axis penetration depth would mirror the observed in-plane linear T dependence, if the c -axis coupling is coherent with a constant matrix element t_\perp . However, studies^{5,6} of atomic overlaps between CuO_2 planes through which c -axis tunneling occurs, have shown that the chemistry involved leads to a matrix element $t(\phi)$ which has d -wave symmetry and is given by $t_\phi \cos^2(2\phi)$, where ϕ gives the direction of the momentum \mathbf{k} in the 2-dimensional CuO_2 Brillouin zone. In general, there could be a contribution from both a constant t_\perp and $t(\phi)$. For the case of $t(\phi)$, the low T dependence of the resulting $\rho_s(T)$ for a d -wave superconductor is T^5 (See Ref.⁵). Such a dependence on T has been observed in a recent experiment⁷ on Bi2212 indicating that $t(\phi)$ is the dominant coherent matrix element. While this experiment favors a T^5 , some small contribution from a constant t_\perp and from some incoherent transfer, which gives a T^3 law,^{4,8} cannot be ruled out. In fact, there is strong evidence from the c -axis quasiparticle tunneling work⁹ on mesa junctions of Bi2212 that there is a significant t_\perp part in the coherent matrix element.¹⁰

In this paper we investigate the effect of an in-plane magnetic field \mathbf{H} on the c -axis sum rule and on the corresponding superfluid density. The aim is to see if additional information on the nature of the c -axis coupling can be obtained from such experiments. We consider a general coherent c -axis coupling matrix element [$t_{\perp}(\mathbf{k}) = t_{\perp} + t_{\phi} \cos^2(2\phi)$] as well as impurity mediated transfer from plane to plane.

We begin with the Hamiltonian $\mathcal{H} = H_0 + H_c$, where H_0 describes a d -wave superconductor in the plane and H_c gives the c -axis coupling from plane to plane $H_c = \sum_{\sigma, \mathbf{k}, \mathbf{p}} t_{\mathbf{k}-\mathbf{p}} [C_{1\sigma}^+(\mathbf{k})C_{2\sigma}(\mathbf{p}) + h.c.]$, where $C_{i\sigma}^+(\mathbf{k})$ creates an electron in plane i of momentum \mathbf{k} and spin σ , and $t_{\mathbf{k}-\mathbf{p}}$ is the hopping amplitude between plane 1 and 2. For coherent coupling, $t_{\mathbf{k}-\mathbf{p}} = \delta_{\mathbf{k}-\mathbf{p}} t_{\perp}(\mathbf{k})$. For impurity assisted hopping $t_{\mathbf{k}-\mathbf{p}} = V_{\mathbf{k}-\mathbf{p}}$, where $V_{\mathbf{k}-\mathbf{p}}$ is the impurity potential, and in-plane momentum is not conserved once a configuration average over impurities is carried out.

Consideration of c -axis electrodynamics leads directly to a relation for the superfluid density ρ_s ; namely, $\rho_s = \Delta N + K$ with the missing area $\Delta N = 8 \int_0^{\omega_c} d\omega [\sigma_{1c}^n(\omega) - \sigma_{1c}^s(\omega)]$ and $K = -4\pi e^2 d [\langle H_c \rangle^s - \langle H_c \rangle^n]$, where the cutoff (ω_c) is to be applied at the energy of the interband transitions and $\sigma_{1c}^{n(s)}(\omega)$ is the real part of the c -axis optical conductivity in normal(n) and superconducting(s) state, and e and d are the electron charge and the interlayer spacing, respectively. The difference in c -axis kinetic energy between superconducting and normal state [$\langle H_c \rangle^s - \langle H_c \rangle^n$] gives the correction to the conventional sum rule for which the kinetic energy difference vanishes.

The effect of an in-plane magnetic field on the c -axis kinetic energy difference can be expressed in terms of the Green's function $G(\mathbf{k}, \omega)$ and the corresponding Gorkov function $F(\mathbf{k}, \omega)$. We assume that the field penetrates freely into the sample so that it is uniform between CuO_2 planes.¹⁰ First, we consider the case of coherent c -axis coupling $t_{\perp}(\mathbf{k})$. The c -axis kinetic energy is

$$\begin{aligned} \langle H_c \rangle_{\mathbf{q}}^s &= 4T \sum_{\omega} \sum_{\mathbf{k}} t_{\perp}(\mathbf{k})^2 [G(\mathbf{k} + \mathbf{q}, \tilde{\omega})G(\mathbf{k}, \tilde{\omega}) - F(\mathbf{k} + \mathbf{q}, \tilde{\omega})F(\mathbf{k}, \tilde{\omega})] \\ &\simeq -4TN(0) \sum_{\omega} \int \frac{d\phi}{2\pi} t_{\perp}(\mathbf{k})^2 \int_{-\omega_c}^{\omega_c} d\xi \frac{\tilde{\omega}^2 - \xi(\xi + \epsilon_{\mathbf{q}}) + \Delta_{\mathbf{k}}^2}{[\tilde{\omega}^2 + \xi^2 + \Delta_{\mathbf{k}}^2][\tilde{\omega}^2 + (\xi + \epsilon_{\mathbf{q}})^2 + \Delta_{\mathbf{k}}^2]}, \end{aligned} \quad (1)$$

where $\tilde{\omega} = \omega + \gamma \text{sgn}\omega$ with fermionic Mastubara frequency ω , γ is an effective impurity scattering rate modeled as a constant for simplicity, and $\mathbf{q} = (ed/2)\hat{\mathbf{z}} \times \mathbf{H}$ with $\hat{\mathbf{z}}$ a unit vector along the c -axis. The Green's functions in Eq. (1) with $\mathbf{k} + \mathbf{q}$ involve the quasiparticle energy $E_{\mathbf{k}+\mathbf{q}} \simeq \sqrt{\xi_{\mathbf{k}+\mathbf{q}}^2 + \Delta_{\mathbf{k}}^2}$ with $\xi_{\mathbf{k}+\mathbf{q}} \simeq \xi_{\mathbf{k}} + \epsilon_{\mathbf{q}}$.¹¹ Here, $\xi_{\mathbf{k}}$ is energy spectrum measured with respect to the Fermi energy and $\epsilon_{\mathbf{q}} = qv_F \cos(\phi - \theta_q)$ with the Fermi velocity v_F and θ_q the direction of \mathbf{q} . Note that $\theta_q = \theta + \pi/2$ can be interpreted as the direction of \mathbf{H} (θ) because of the symmetry in the problem.

The difference $\langle H_c \rangle_{\mathbf{q}}^s - \langle H_c \rangle^s$ turns out to be, after some algebra,

$$\langle H_c \rangle_{\mathbf{q}}^s - \langle H_c \rangle^s \simeq \frac{N(0)}{3} \int \frac{d\phi}{2\pi} t_{\perp}(\mathbf{k})^2 \left(\frac{\omega_c}{T} \right)^2 \tanh \left(\frac{\omega_c}{2T} \right) \left[\tanh \left(\frac{\omega_c}{2T} \right)^2 - 1 \right] \left(\frac{\epsilon_{\mathbf{q}}}{\omega_c} \right)^2. \quad (2)$$

The correction to Eq. (2) is $\mathcal{O}[(v_F q/\omega_c)^2(\Delta_0/\omega_c)^2]$. Note that $(v_F q/\omega_c)^2$ is negligible and, furthermore, the quantity in the square bracket vanishes since $T \ll \omega_c$. The same holds in the normal state *i.e.* $\langle H_c \rangle_{\mathbf{q}}^n - \langle H_c \rangle^n \simeq 0$. Consequently, the kinetic energy difference between superconducting and normal state does not change with in-plane magnetic field. For incoherent coupling, the same conclusion applies but for simpler reason. In this case

$$\langle H_c \rangle_{\mathbf{q}}^s \simeq 4TN(0) \sum_{\omega} \int \frac{d\phi_k d\phi_p}{(2\pi)^2} |V(\phi_k, \phi_p)|^2 \int d\xi_{\mathbf{k}} d\xi_{\mathbf{p}} \Phi(\xi_{\mathbf{k}} + \epsilon_{\mathbf{q}}, \Delta_{\mathbf{k}}) \Phi(\xi_{\mathbf{p}}, \Delta_{\mathbf{p}}), \quad (3)$$

where $\Phi(\xi, \Delta) = (i\tilde{\omega} + \xi - \Delta) / (\tilde{\omega}^2 + \xi^2 + \Delta^2)$. By changing $\xi_{\mathbf{k}} + \epsilon_{\mathbf{q}} \rightarrow \xi_{\mathbf{k}}$, we see that $\langle H_c \rangle_{\mathbf{q}}^s = \langle H_c \rangle^s$, and there is no change in kinetic energy.

The superfluid density ρ_s is $\rho_s = \Delta N + K$. In the presence of an in-plane field, the superfluid density ($\rho_{s,\mathbf{q}}$) becomes $\Delta N_{\mathbf{q}} + K_{\mathbf{q}}$, where $\rho_{s,\mathbf{q}} = \rho_s + \delta\rho_s$, $\Delta N_{\mathbf{q}} = \Delta N + \delta\Delta N$, and $K_{\mathbf{q}} = K + \delta K$. Since $\delta K = 0$, we find $\delta\rho_s = \delta\Delta N$. The conductivity sum rule (or the normalized missing spectral weight) is

$$\frac{\Delta N_{\mathbf{q}}}{\rho_{s,\mathbf{q}}} = \frac{\Delta N + \delta\Delta N}{\rho_s + \delta\rho_s} \simeq \frac{\Delta N}{\rho_s} + \frac{\delta\rho_s}{\rho_s} \left[1 - \frac{\Delta N}{\rho_s} \right]. \quad (4)$$

For pure coherent coupling, $\Delta N/\rho_s = 1$, and for pure incoherent coupling, $\delta\rho_s = 0$; therefore, the sum rule is not changed by \mathbf{H} . However, if both are present, the sum rule is changed because $\delta\rho_s \neq 0$ from the coherent contribution, and $\Delta N/\rho_s \neq 1$ from the incoherent part.³

We next compute the change in superfluid density in the presence of \mathbf{H} only for coherent coupling because \mathbf{H} has no effect for incoherent coupling. For a constant t_\perp , the superfluid density $\rho_{s,\mathbf{q}}$ is $\rho_{s,\mathbf{q}} = t_\perp^2 \mathcal{C} T \sum_\omega \sum_{\mathbf{k}} F(\mathbf{k} + \mathbf{q}, \tilde{\omega}) F(\mathbf{k}, \tilde{\omega})$, where $\mathcal{C} = 16\pi e^2 d$. Assuming a cylindrical Fermi surface, we obtain, as $T \rightarrow 0$,

$$\rho_{s,\mathbf{q}} = t_\perp^2 \mathcal{C} N(0) \int \frac{d\phi}{2\pi} \frac{\Delta_{\mathbf{k}}^2}{\epsilon_{\mathbf{q}} \sqrt{4\Delta_{\mathbf{k}}^2 + \epsilon_{\mathbf{q}}^2}} \ln \left[\frac{\Psi_+^{(1)} \Psi_-^{(2)}}{\Psi_-^{(1)} \Psi_+^{(2)}} \right], \quad (5)$$

where $\Psi_\pm^{(1)} = \sqrt{4\Delta_{\mathbf{k}}^2 + \epsilon_{\mathbf{q}}^2} \pm \epsilon_{\mathbf{q}}$ and $\Psi_\pm^{(2)} = \sqrt{4\Delta_{\mathbf{k}}^2 + \epsilon_{\mathbf{q}}^2} \sqrt{\Delta_{\mathbf{k}}^2 + \gamma^2} \pm \gamma \epsilon_{\mathbf{q}}$. At finite T with $\gamma = 0$, we obtain

$$\rho_{s,\mathbf{q}}(T) = t_\perp^2 \mathcal{C} \sum_{\mathbf{k}} \frac{\Delta_{\mathbf{k}}^2 [\chi(E_{\mathbf{k}}) - \chi(E_{\mathbf{k}+\mathbf{q}})]}{2(E_{\mathbf{k}+\mathbf{q}}^2 - E_{\mathbf{k}}^2)}, \quad (6)$$

where $\chi(E) = \tanh(E/2T)/E$. For general coherent coupling, we simply replace t_\perp^2 by $t_\perp(\mathbf{k})^2$ within the sum over \mathbf{k} . As $\mathbf{H} \rightarrow 0$, $\rho_{s,\mathbf{q}}(T) \rightarrow \rho_s(T)$. Applying the nodal approximation¹² to the general case for $T \ll \Delta_0$, we obtain, at $\mathbf{H} = 0$, for a pure case $\rho_s(T) = \rho_s(0) - \mathcal{C} N(0) [\alpha_1 t_\perp^2 (T/\Delta_0) + \alpha_3 t_\perp t_\phi (T/\Delta_0)^3 + \alpha_5 t_\phi^2 (T/\Delta_0)^5]$, where $[\alpha_1, \alpha_3, \alpha_5] = [\ln(2), 4.48\zeta(3), 42.2\zeta(5)]$. The t_\perp^2 contribution is linear in T as expected and the t_ϕ^2 goes like T^5 , a well known result.⁵ The $t_\perp t_\phi$ cross term gives T^3 just as does the impurity mediated contribution.⁸ In the above expression, $\rho_s(0) = \mathcal{C} N(0) [t_\perp^2/2 + t_\perp t_\phi/2 + 3t_\phi^2/16]$. From here on we will use the notation $\rho_{s,\mathbf{q}}^{(i)}$ with $i = 1, 2$, and 3 for t_\perp^2 , $t_\perp t_\phi$, and t_ϕ^2 contribution, respectively.

Numerical results for $\rho_{s,\mathbf{q}}^{(i)}/\rho_s^{(i)}(0)$ as a function of ϵ_q/T_c with $\theta_q = 0$ and $\gamma = 0$ are given in Fig. (1). One should not confuse $\epsilon_q (\equiv qv_F)$ with $\epsilon_{\mathbf{q}} = \epsilon_q \cos(\phi - \theta_q)$. The curve labeled (1) refers to the t_\perp^2 contribution and is nearly a straight line implying a linear dependence on H (the magnitude of \mathbf{H}). For $t(\phi)^2 = t_\phi^2 \cos^4(2\phi)$, the effect of the field on $\rho_{s,\mathbf{q}}^{(3)}/\rho_s^{(3)}(0)$ is now much smaller than for t_\perp^2 as the curve (3) shows. This reduction results because the nodal quasiparticles are eliminated from the c -axis transport in this case by the factor $\cos^4(2\phi)$. The numerical data for the t_ϕ^2 case fit well an H^2 law at small H . The last curve in Fig. (1) which is labeled by (2) refers to the cross term $2t_\perp t_\phi \cos^2(2\phi)$. It also fits an H^2 . Thus the

constant t_{\perp} part in $t_{\perp}(\mathbf{k})$ is most effective in producing a change in $\rho_{s,\mathbf{q}}$ in the presence of \mathbf{H} .

It is instructive to derive an approximate, but analytic expression at $T = 0$, for the \mathbf{H} dependence of $\rho_{s,\mathbf{q}}$ just discussed. We start from the temperature-independent part of Eq. (6). Applying a nodal approximation¹² should be reasonable for the difference between $\rho_{s,\mathbf{q}}$ and $\rho_s(0)$. In this approximation, $\sum_{\mathbf{k}} \rightarrow \sum_{\text{node}} \int \mathcal{J} p dp d\vartheta$, where $\mathcal{J} = [(2\pi)^2 v_F v_G]^{-1}$ after an appropriate coordinate transformation. The integration over p is to be limited to the nodal region with cutoff p_0 of order Δ_0 . The quasiparticle energy $E_{\mathbf{k}} = \sqrt{\xi_{\mathbf{k}}^2 + \Delta_{\mathbf{k}}^2}$ then takes the form $E_{\mathbf{k}} = \sqrt{p_1^2 + p_2^2} = p$, where $p_1 = p \cos(\vartheta)$ and $p_2 = p \sin(\vartheta)$. In \mathcal{J} , $1/(\pi v_F v_G) = N(0)/\Delta_0$ with $N(0)$ the density of states at the FS. Near a node we can approximate $\epsilon_{\mathbf{q}} \simeq \epsilon_q \cos(\phi_n - \theta_q)$, where $\phi_n = \pi/4, 3\pi/4, 5\pi/4$, or $7\pi/4$. Thus for a give value of θ_q , say $\theta_q = 0$, $\epsilon_{\mathbf{q}} \simeq \pm \epsilon_q / \sqrt{2}$.

For the t_{\perp}^2 case, choosing $\theta_q = 0$, that is \mathbf{H} along an anti-node, applying the nodal approximation we obtain $\rho_{s,\mathbf{q}}^{(1)}/\rho_s^{(1)}(0) = 1 - (\pi/8\sqrt{2})(\epsilon_q/\Delta_0)$, where $\rho_s^{(1)}(0) = t_{\perp}^2 \mathcal{C} N(0)/2$. We choose $\Delta_0 = 2.14 T_c$, then $\rho_{s,\mathbf{q}}^{(1)}/\rho_s^{(1)}(0) = 1 - (\epsilon_q/T_c)/7.71$. Comparison with our numerical result given in Fig. (1) shows that this simple expression works well up to $\epsilon_q = 0.5 T_c$. Similarly, for both $t(\phi)^2$ and $t_{\perp} t(\phi)$ term, we obtain $\rho_{s,\mathbf{q}}^{(i)}/\rho_s^{(i)}(0) \simeq 1 - (\epsilon_q/\Delta_0)^2/4$, where $i = 2$ and 3 . Consequently, in the presence of the in-plane magnetic field along the anti-node, the ϵ_q dependence of $\rho_{s,\mathbf{q}}$ is $|\epsilon_q|$ for the t_{\perp}^2 term, and ϵ_q^2 for both $t_{\perp} t(\phi)$ and $t(\phi)^2$ terms. Even if \mathbf{H} is in the nodal direction, the ϵ_q dependence of $\rho_{s,\mathbf{q}}$ does not change; however, the coefficient of $|\epsilon_q|$ (or ϵ_q^2) becomes smaller because the field has no effect on the quasiparticle with $\phi_n \simeq \theta \pm \pi/2$.

While in Fig. (1) we took the field along the anti-nodal direction, in Fig. (2) we show additional results as a function of θ in the range 0 to π for specific values of ϵ_q . The pattern obtained has four fold symmetry for a d -wave gap. Note that the underlying symmetry of the problem ensures that $\rho_{s,\mathbf{q}}$ is periodic in $\pi/2$ as is the quasiparticle conductivity.¹⁰ The thin solid line is for a constant t_{\perp}^2 with $\epsilon_q = 0.1T_c$, $\gamma = 0$, and $T = 0$ while the thick solid line is for $\epsilon_q = 0.2T_c$ (higher magnetic field). At all angle θ , $\rho_{s,\mathbf{q}}$ is reduced over its zero field

value. There is a minimum along the anti-nodal direction and a maximum along the nodal direction. In fact, for \mathbf{H} along the node it can be shown by an application of the nodal approximation that $\rho_{s,\mathbf{q}}^{(1)}/\rho_s^{(1)}(0) = 1 - (\pi/16)\epsilon_q/\Delta_0$. Note that the ratio of anti-nodal to nodal reduction in $\rho_{s,\mathbf{q}}$ is $\sqrt{2}$ which is verified in our complete numerical calculations. This happens because the superfluid density depends on $|\epsilon_q|$ for a constant hopping amplitude.

Temperature and impurities will have an effect on the four fold symmetry pattern shown in Fig. (2). The first short dashed curve is for $\rho_{s,\mathbf{q}}^{(1)}(T)$ with $\gamma = 0$ but now $T = 0.001 T_c$ while the second is for $T = 0.01 T_c$. Both are to be compared with the $T = 0$ result (thin solid curve). We see that in the first case T simply rounds off a little the maxima in the nodal directions while for a higher $T = 0.01 T_c$, which is still much less than the magnetic energy $\epsilon_q = 0.1 T_c$, the temperature effects are more significant and much of the anisotropy is washed out. To see the anisotropy, which comes only from t_{\perp}^2 , one clearly needs to go to low temperature compared to the magnetic energy. Impurities also affect the anisotropy of $\rho_{s,\mathbf{q}}$ and results for $\gamma = 0.002 T_c$ are shown as the long dashed curve in Fig. (2). These results are to be compared with the thick solid curve which applies for the same value of $\epsilon_q = 0.2 T_c$. Impurities reduces the c -axis superfluid density as we expect, and smears out the anisotropy. The final dot-dashed line in Fig. (2) is for the term $t(\phi)^2$ with $\epsilon_q = 0.1 T_c$ and $\gamma = 0$. The superfluid reduction is small in comparison to the other curves and shows no anisotropy.

More information on the effect of temperature, impurities and the magnetic field on the superfluid density for the t_{\perp}^2 case is given in Fig. (3). All curves are for the field along the anti-node (except the solid curve in the lower inset, which is for the field along the node). The solid curve is for comparison and gives the T dependence of $\rho_s^{(1)}(T)/\rho_s^{(1)}(0)$ with $\mathbf{H} = 0$. The other curves are for different increasing values of $\epsilon_q/T_c = 0.1$ (dashed), 0.2 (dot-dashed), and 0.3 (long dashed curve). At low T , the power law in T is modified going to a T^3 while at high T it returns to T . It is seen that T always decreases the superfluid density as does ϵ_q . In all our finite T numerical results, we have approximated the T dependence of the gap

amplitude $\Delta(T)$ by $\Delta_0 \tanh \left[1.74 \sqrt{(T/T_c) - 1} \right]$. In the top inset we show similar results but as functions of magnetic energy ϵ_q/T_c for different values of γ/T_c at $T = 0$. The solid curve is for $\gamma/T_c = 0$, with which we compare other curves for $\gamma/T_c = 0.01$ (dashed), 0.02 (dot-dashed), and 0.03 (long dashed curve). Impurities, like T , have their greatest effect at $\epsilon_q = 0$.

We can obtain analytic results for the T dependence of $\rho_{s,\mathbf{q}}(T) = \rho_{s,\mathbf{q}} + \delta\rho_{s,\mathbf{q}}(T)$. We start with the constant t_{\perp}^2 case. Applying the nodal approximation already described, when the field is along an anti-node we obtain $\delta\rho_{s,\mathbf{q}}^{(1)}(T)/\rho_s^{(1)}(0) = -12\zeta(3) (T/\Delta_0) (T/\epsilon_q)^2$. For the $t(\phi)^2$ term, we obtain $\delta\rho_{s,\mathbf{q}}^{(3)}(T)/\rho_s^{(3)}(0) \simeq -9450\zeta(7) (T/\epsilon_q)^2 (T/\Delta_0)^5$, which goes like T^7 . Similarly, we have, for $t_{\perp}t(\phi)$, $\delta\rho_{s,\mathbf{q}}^{(2)}(T)/\rho_s^{(2)}(0) \simeq -270\zeta(5) (T/\epsilon_q)^2 (T/\Delta_0)^3$, which gives T^5 . For incoherent coupling, $\rho_{s,\mathbf{q}}(T) = \rho_s(T)$ and its dependence remains T^3 as shown in Ref.⁸ For coherent coupling, \mathbf{H} along an anti-node changes the T dependence of the superfluid density as follows: $\rho_{s,\mathbf{q}}(T) \sim T^2\rho_s(T)$. If $\theta \simeq \phi_n$, say $\theta \simeq \pi/4$, then $\epsilon_{\mathbf{q}} \simeq 0$ for $\phi_n = 3\pi/4, 7\pi/4$. This means that the in-plane field has no effect on quasiparticles with $\phi_n = 3\pi/4, 7\pi/4$. Consequently, $\rho_{s,\mathbf{q}}(T) \sim \rho_s(T)$ for \mathbf{H} along a node. This is shown in the lower inset of Fig. (3). The solid curve is for the nodal direction while the dashed curve is along the anti-node. The anisotropy disappears for $T > 0.1 T_c$.

It is clear from our analysis that a contribution to $\rho_{s,\mathbf{q}}$ from a small t_{\perp}^2 term will lead to anisotropy in $\rho_{s,\mathbf{q}}$ as a function of the orientation of \mathbf{H} , and be linear in H for small field. In the pure case, its dependence is linear in T going over to T^3 at finite field along an anti-node with $T < \epsilon_q$ (magnetic energy). These characteristic variation are quite distinct from those predicted for a $t(\phi)^2$ term or for the cross term $t_{\perp}t(\phi)$. In both these cases there is no anisotropy at $T = 0$ and the changes with \mathbf{H} are quadratic (ϵ_q^2). In the pure case with zero field, the T variations are T^5 and T^3 , respectively, and go over to T^7 and T^5 at finite field for $T < \epsilon_q$. These characteristic laws should help constraint further the relative magnitude of t_{\perp} , t_{ϕ} and also of incoherent coupling. In this last instance, there is no effect of \mathbf{H} and the T^3 remains at finite field and low T .

In conclusion, we have considered the effect of an in-plane magnetic field \mathbf{H} on the c -axis sum rule and superfluid density($\rho_{s,\mathbf{q}}$). We have assumed that the in-plane dynamics can be described within a Fermi liquid theory. If the c -axis coupling is coherent, the sum rule remains conventional and unaffected by the application of \mathbf{H} but $\rho_{s,\mathbf{q}}$ itself is reduced with increasing \mathbf{H} . The reduction with \mathbf{H} depends on the exact functional form of the c -axis coherent coupling and is different for a constant matrix element t_{\perp} and $t(\phi) = t_{\phi} \cos^2(2\phi)$. In the first instance, to leading order, it varies like H (magnitude of \mathbf{H}) while in the second like H^2 . If, however, the c -axis transport is incoherent, then both the sum rule and $\rho_{s,\mathbf{q}}$ remains unchanged. When both coherent and incoherent interlayer transfer contribute, both the sum rule and $\rho_{s,\mathbf{q}}$ will change with \mathbf{H} . The change in $\rho_{s,\mathbf{q}}$ comes only from the coherent part.

For the case of coherent c -axis coupling with a constant t_{\perp} , the change in $\rho_{s,\mathbf{q}}$ depends on the direction of \mathbf{H} with respect to the nodes. For \mathbf{H} along an anti-nodal direction $\rho_{s,\mathbf{q}}$ is minimum while it has a sharp maximum when \mathbf{H} is along a nodal direction. This anisotropy in $\rho_{s,\mathbf{q}}$ is reduced when impurities are present or when the temperature is increased. For the case of $t(\phi)$, the contribution to the transport coming from the nodes is eliminated and the anisotropy disappears. The incoherent coupling contribution also gives an isotropic response because in this case momentum is not conserved and, correspondingly, the momentum shift caused by \mathbf{H} is immaterial.

REFERENCES

- ¹ R. A. Ferrell and R. E. Glover, Phys. Rev. **109**, 1398 (1958); M. Tinkham and R. A. Ferrell, Phys. Rev. Lett. **2**, 331 (1959).
- ² D. N. Basov *et al.*, Science **283**, 49 (1999); A. S. Katz *et al.*, Phys. Rev. B **61**, 5930 (2000).
- ³ W. Kim and J. P. Carbotte, Phys. Rev. B **61**, R11886 (2000); *ibid* **62**, 8661 (2000).
- ⁴ R. J. Radtke *et al.*, Phys. Rev. B **53**, R522 (1996).
- ⁵ T. Xiang and J. M. Wheatley, Phys. Rev. Lett. **77**, 4632 (1996).
- ⁶ K. G. Sandeman and A. J. Schofield, cond-mat/0007299.
- ⁷ M. B. Gaifullin *et al.*, Phys. Rev. Lett. **83**, 3928 (1999).
- ⁸ P. J. Hirschfeld *et al.*, Phys. Rev. B **55**, 12 742 (1997).
- ⁹ Y. I. Latyshev *et al.*, Phys. Rev. Lett. **82**, 5345 (1999).
- ¹⁰ W. Kim and J. P. Carbotte, submitted to PRB; cond-mat/0010314.
- ¹¹ The gap seen by quasiparticles with $\mathbf{k} + \mathbf{q}$ is not $\Delta_{\mathbf{k}}$ but $\Delta_{\mathbf{k}+\mathbf{q}}$; however, this difference can be neglected in our calculation. See Ref.¹⁰
- ¹² P. A. Lee, Phys. Rev. Lett. **71**, 1887 (1993); A. C. Durst and P. A. Lee, cond-mat/9908182.

FIGURES

FIG. 1. $\rho_{s,\mathbf{q}}^{(i)}/\rho_s^{(i)}(0)$ as functions of ϵ_q/T_c for $T = 0$, $\theta = 0$ and $\gamma = 0$. Note that the superscripts (1), (2) and (3) represent t_\perp^2 , $t_\perp t_\phi$ and t_ϕ^2 , respectively.

FIG. 2. $\rho_{s,\mathbf{q}}^{(i)}/\rho_s^{(i)}(0)$ as functions of θ . The dot-dashed line is for t_ϕ^2 with $\epsilon_q = 0.1T_c$, $\gamma = 0$, and $T = 0$. The thin solid curve is for t_\perp^2 with $\epsilon_q = 0.1T_c$, $\gamma = 0$, and $T = 0$. The two dashed curves just below this curve are for t_\perp^2 with $\gamma = 0$, and $T = 0.001T_c$ and $T = 0.01T_c$, respectively. The thick solid curve is for the case of t_\perp^2 with $\epsilon_q = 0.2T_c$, $\gamma = 0$, and $T = 0$. The long-dashed curve is for $\epsilon_q = 0.2T_c$, $\gamma = 0.002T_c$, and $T = 0$.

FIG. 3. $\rho_{s,\mathbf{q}}^{(1)}/\rho_s^{(1)}(0)$ as functions of T/T_c for different values of ϵ_q/T_c with $\theta = 0$ and $\gamma = 0$ (pure case). The solid curve is for $\epsilon_q/T_c = 0$ (zero field). The dashed, dot-dashed, and long-dashed curve for $\epsilon_q/T_c = 0.1, 0.2$, and 0.3 , respectively. In the upper inset, $\rho_{s,\mathbf{q}}^{(1)}/\rho_s^{(1)}(0)$ is given as functions of ϵ_q/T_c for different values of γ/T_c with $\theta = 0$ and $T = 0$. The solid, dashed, dot-dashed, and long-dashed curve for $\gamma/T_c = 0, 0.01, 0.02$, and 0.03 , respectively. In the lower inset, $\rho_{s,\mathbf{q}}^{(1)}/\rho_s^{(1)}(0)$ as functions of T/T_c for $\epsilon_q = 0.3 T_c$. The solid curve is for $\theta \simeq \pi/4$ and the long-dashed curve for $\theta = 0$.

Fig. 1

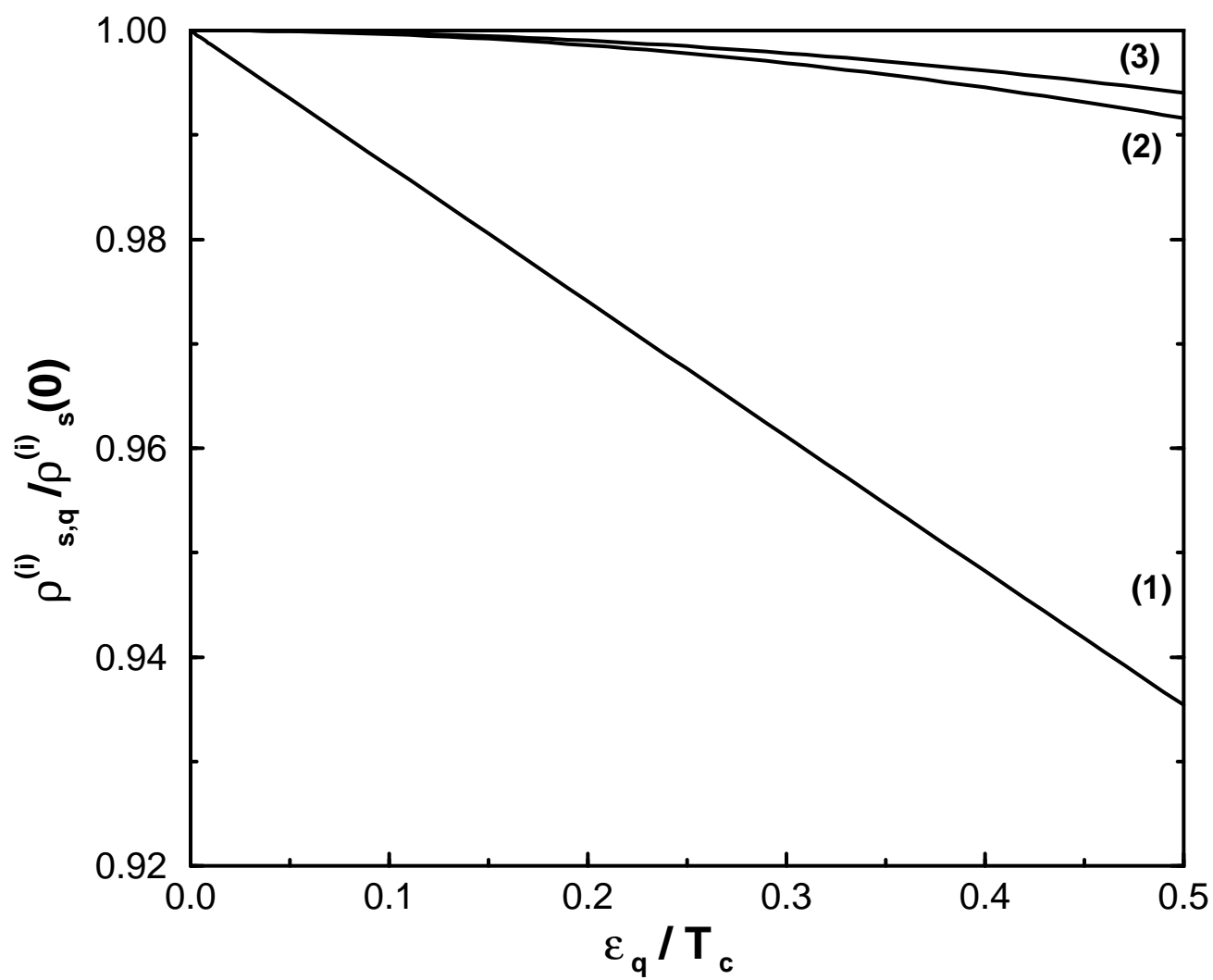


Fig.2

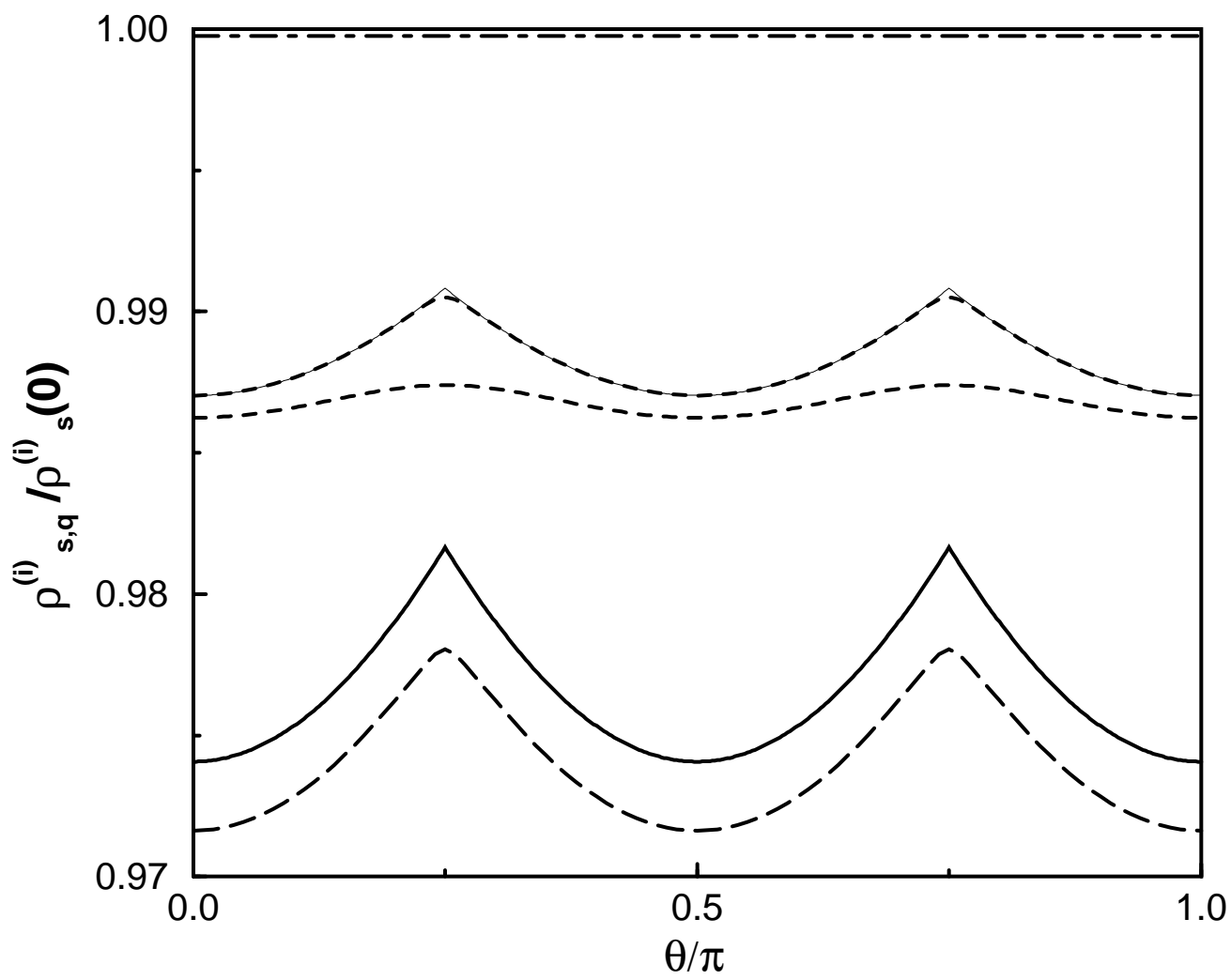


Fig.3

